



## Article

# Effect of the Testing Temperature on the Impact Property of a Multilayered Soft–Hard Copper–Brass Block

Tong Liu <sup>1,2</sup> , Jiansheng Li <sup>1,2,\*</sup>, Kezhang Liu <sup>1</sup>, Mengmeng Wang <sup>1,2</sup>, Yu Zhao <sup>1,2,3,\*</sup>, Zhongchen Zhou <sup>4</sup>, Yong Wei <sup>1</sup>, Qi Yang <sup>1</sup>, Ming Chen <sup>1</sup>, Qingzhong Mao <sup>4,\*</sup>  and Yufeng Sun <sup>1,2</sup>

<sup>1</sup> School of Materials Science and Engineering, Anhui Polytechnic University, Wuhu 241000, China

<sup>2</sup> Anhui Key Laboratory of High-Performance Non-Ferrous Metal Materials, Anhui Polytechnic University, Wuhu 241000, China

<sup>3</sup> NBTM New Materials Group Corporation Limited, Ningbo 315000, China

<sup>4</sup> School of Materials Science and Engineering, Nanjing University of Science and Technology, Nanjing 210094, China

\* Correspondence: lijiansheng@ahpu.edu.cn or drlijiansheng@163.com (J.L.); zhaoyu@ahpu.edu.cn (Y.Z.); 216116000150@njust.edu.cn (Q.M.)

**Abstract:** The impact property is one of the most significant mechanical properties for metallic materials. In the current work, a soft–hard copper–brass block with a high yield strength of ~320 MPa and good uniform elongation of ~20% was prepared, and the effect of the testing temperature on its impact property was explored. The results showed that the impact energy was decreased with the increase in testing temperature. The impact energies at liquid nitrogen temperature (LNT), room temperature (RT), and 200 °C were 8.15 J, 7.39 J, and 7.04 J, respectively. The highest impact energy at LNT was attributed to the coordinated plastic deformation effects, which was indicated by the tiny dimples during the process of the delamination of soft–hard copper–brass interfaces. The high temperature of 200 °C can weaken the copper–brass interface and reduce the absorption of deformation energy, result in low impact energy.

**Keywords:** copper–brass block; testing temperature; impact property; multilayered structure; delamination



**Citation:** Liu, T.; Li, J.; Liu, K.; Wang, M.; Zhao, Y.; Zhou, Z.; Wei, Y.; Yang, Q.; Chen, M.; Mao, Q.; et al. Effect of the Testing Temperature on the Impact Property of a Multilayered Soft–Hard Copper–Brass Block. *Coatings* **2022**, *12*, 1236. <https://doi.org/10.3390/coatings12091236>

Academic Editor: Alexandru Enesca

Received: 29 July 2022

Accepted: 20 August 2022

Published: 24 August 2022

**Publisher's Note:** MDPI stays neutral with regard to jurisdictional claims in published maps and institutional affiliations.



**Copyright:** © 2022 by the authors. Licensee MDPI, Basel, Switzerland. This article is an open access article distributed under the terms and conditions of the Creative Commons Attribution (CC BY) license (<https://creativecommons.org/licenses/by/4.0/>).

## 1. Introduction

Pure copper and copper alloys are widely applied in thermal conductive devices and electronic equipment because of their superior thermal and electrical properties [1,2]. However, the low yield strength of pure copper and its alloys, especially for their coarse-grained states, may limit their application as structural parts in thermal and electrical applications [3–5]. Severe plastic deformation can turn the coarse-grained structures into ultrafine or nano-grained structures, which will greatly enhance the strength of pure copper and its alloys [6–8]. However, the toughness was dramatically reduced by the defects formed in the deformed structures, and thus increased the risk of catastrophic failure of mechanical parts [5,9]. Fabricating/processing copper and its alloys with high strength and good toughness was also expected by scientists and engineers, which will further broaden their industrial applications.

As studied from the literatures in the past several years, designing the dissimilar-metal blocks with multilayered soft–hard structures can be effectively realized by high pressure torsion + rolling + annealing [10,11], accumulative roll bonding [12,13] and hot pressing + hot rolling + annealing [14]. Multilayered soft–hard structures usually exhibited a good combination of strength and toughness. [15–17]. The enhanced strength was attributed to hetero-deformation induced hardening caused by extra geometrically necessary dislocations accumulated around deformed soft–hard interfaces [10–13,16,18]. The superior impact toughness was explained by that lots of crack deflection or interfacial delamination

was formed by high-speed impacting load. These crack deflection or interfacial delamination usually consumed huge energy and impeded crack propagation [17,19]. Recently, Ma et al. [10,12] and Li et al. [15–17] have successfully fabricated novel multilayered soft-hard copper–brass blocks with high yield strength as well as superior impact toughness. Many efforts were devoted to explore the influence factors of strengthening mechanisms for soft-hard copper–brass blocks, such as layer thickness, interfacial bonding strength and hardness ration of soft-hard layer [10–13,16]. However, there was scarce exploration of the fracture behavior and toughening mechanism for soft-hard copper–brass blocks. Our recent work indicated that the structural orientation had an important influence on Charpy impact toughness of soft-hard copper–brass block [17]. The Charpy impact toughness tested along the vertical orientation was superior to that test along the parallel orientation. This enhanced impact resistance along the vertical orientation was related to the coordination deformation behavior around copper–brass interfaces [17]. As a matter of fact, many factors could affect the impact toughness for soft-hard copper–brass blocks. Service temperature is one of typical factors that should be paid attention. As reported by previous works [20,21], the face-centered-cubic (FCC) metals usually exhibited slightly variation of impact toughness as the decreasing of testing temperature. This was because of that the impact resistance of FCC metals was usually insensitive to the environmental temperature. For multilayered soft-hard copper–brass blocks, there was a typical feature of many soft-hard interfaces. Up to now, the impact behavior of soft-hard interface under low and high temperatures was not revealed for copper–brass blocks. Impact toughness of the copper–brass blocks was believed to be affected by deformation behaviors of soft-hard interfaces, and it should also be paid more attentions.

In present work, a multilayered soft-hard copper–brass block with high yield strength of ~320 MPa and good uniform elongation of ~20% was prepared by a combined processing technique of diffusion welding, forging and annealing (DWFA technique), which had induced in previous work [17]. The influence of testing temperatures on its impact property was studied. Simultaneously, the fracture mechanisms were revealed at liquid nitrogen temperature (LNT), room temperature (RT) and 200 °C.

## 2. Experimental

### 2.1. Materials and Preparation

Commercial ASTM-C11000 copper sheets (99.9 wt% Cu) and ASTM-C26000 brass (Cu-30 wt% Zn) sheets were used in the current work, which were provided by Anhui Xinke New Materials Stock Co., Ltd. The original thicknesses for the copper sheet and brass sheet were 1 mm and 0.8 mm, respectively. Before fabricating a multilayered soft-hard copper–brass block, all of the above sheets were cut with the same dimensions of  $100 \times 150 \text{ mm}^2$ , and then they were polished using SiC paper ( $\Phi 10 \text{ }\mu\text{m}$  for the SiC grit) and washed in an acetone solution for 15 min. Figure 1 shows that a combined DWFA technique was used to prepare the multilayered soft-hard copper–brass blocks. There were four steps in the fabrication processes: (I) 20 layers of copper sheets and 20 layers of brass sheets were stacked at intervals; (II) the stacked copper–brass sheets totaling 40 layers were welded using a diffusion welding machine (ZM-Y, Shanghai Chenhua Electric Furnace Co., Ltd., Shanghai, China) to obtain a copper–brass block, where during the diffusion welding process the stacked copper–brass sheets were extruded under the static pressure of 2 MPa and annealed at 920 °C for 2 h, so as to guarantee the diffusion of Cu/Zn and achieve the metallurgical bonding between the copper and brass sheets; (III) the diffusion-welded copper–brass block was further punched using a pneumatic hammer (C41-75, Nantong Shenwei Forming Machine Works Co., Ltd., Nantong, China), which reduced the thickness from 36 mm to 4 mm and achieved an average layer thickness of ~100  $\mu\text{m}$ ; (IV) the forged copper–brass block was finally annealed at 300 for 2.5 h using a muffle furnace (KSL-1100X, HF-Kejing, Hefei, China). The temperature in the chamber was detected using a K-type thermocouple and the measurement accuracy was  $\pm 1 \text{ }^\circ\text{C}$ . The detailed fabricating processes and related parameters can be also found in Figure 1 and in previous work [17].

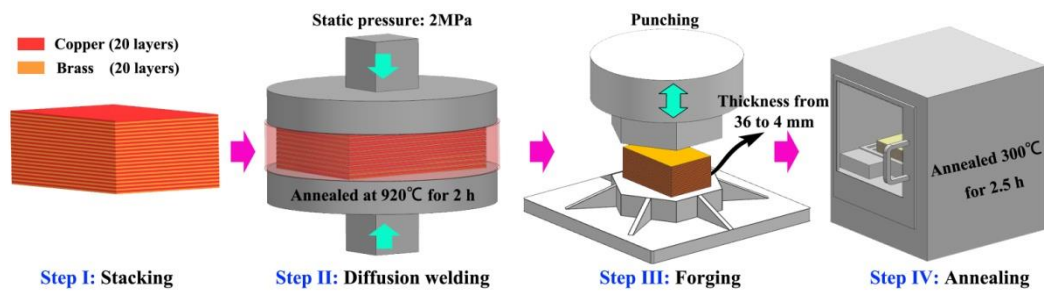


**Figure 1.** A schematic illustration of the fabrication of a multilayered soft–hard copper–brass block. It is noted that the related processing parameters are included in this figure.

## 2.2. Mechanical Tests

The microhardness of the copper–brass block was detected utilizing a Vickers hardness tester (HVM-G 21DT, Shimadzu, Tokyo, Japan). The applied load was 0.98 N, and the holding time was 15 s. Each of the hardness values was obtained by averaging at least 5 indents. The uniaxial tension tests were performed at RT using a universal tension machine (LFM-20, Walter+Bai AG, Löhningen, Switzerland). A typical engineering stress–strain curve of the copper–brass block was captured based on a flat “dog bone” tension sample. Its gauge dimensions were  $5 \times 2.5 \times 2 \text{ mm}^3$ . During the tension experiment, three copper–brass tension specimens were tested to guarantee the reliability of the tensile result at RT, and the strain rate was  $2 \times 10^{-3} \text{ s}^{-1}$ . A Charpy impact tester (PH50/15J, Walter+Bai AG, Löhningen, Switzerland) with a testing module with a maximum capacity of 15 J was utilized to assess the impact energy values of the copper–brass blocks. The measurement resolution was 0.001 J. V-notched Charpy impacting specimens were cut with the dimensions of  $18 \times 4 \times 2 \text{ mm}^3$  (length  $\times$  height  $\times$  thickness  $\text{mm}^3$ ). The detailed specimen dimensions and corresponding images are displayed in Figure 2. In this work, each impact test was performed five times to guarantee the reliability of the data. In order to obtain the various testing temperatures, the impacting specimens were immersed in liquid nitrogen or heated at 200 °C in a furnace for a long time period of 10 min to achieve a specific temperature of  $-196 \text{ °C}$  or 200 °C, respectively. Then, they were immediately taken out for impact testing. All of the above operations were completed within 5 s to guarantee the reliability of the testing temperatures. Detailed information regarding the selection of tension and Charpy impact specimens can be found in Figure 3.

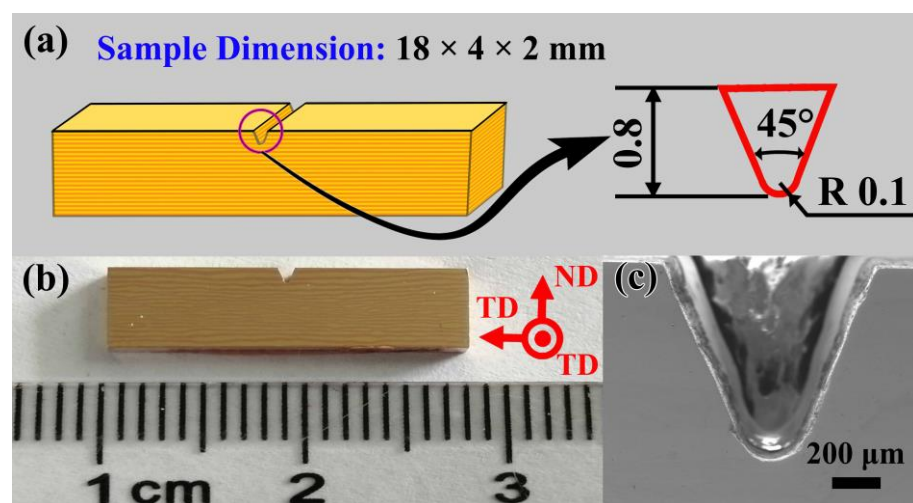


**Figure 2.** (a) The dimensions of the impact specimens in the present work. (b) Impact specimens cut from a multilayered soft–hard copper–brass block. (c) A scanning electron microscope (SEM) image of the V-notch.

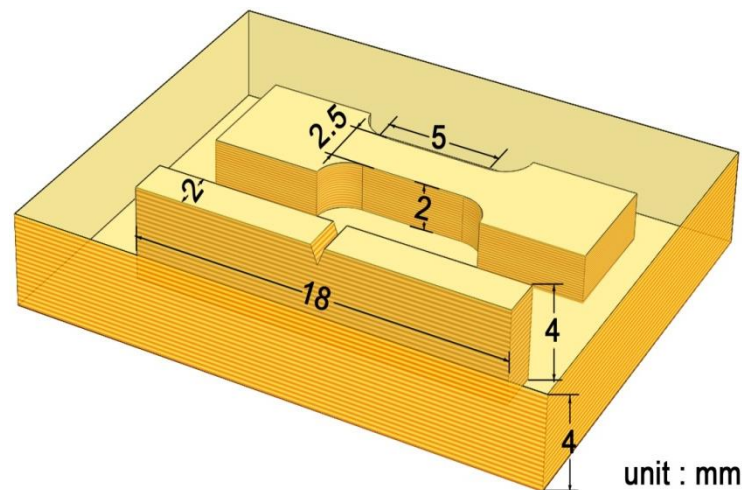


**Figure 3.** Schematic illustration of the selection of a tension sample and Charpy impact sample.

### 2.3. Microstructural Characterization

Macro-images of the untested and tested impact samples were obtained using a Nikon camera. A field emission scanning electron microscope (SEM, Quant 250 FEG, FEI, Hillsboro, OR, USA) with an accelerating voltage of 20 keV was used to capture the fracture morphologies for the Charpy impacting samples impacted at various temperatures. The original and deformed microstructures were analyzed using an electron backscattering diffraction (EBSD) technique, which was conducted on the above SEM machine. The accelerating voltage and step size for the EBSD testing were 15 keV and 200–300 nm, respectively. The EBSD specimens were firstly prepared via mechanical polishing, and then they were polished at 3.8 V in a phosphoric acid (85 mL) + H<sub>2</sub>O (15 mL) solution for 40 s.

### 3. Results and Discussion

Figure 4 presents the microstructure of the multilayered copper–brass block. As can be observed from Figure 4a,b, the copper and brass layers exhibit a diverse structure. The copper layer shows a deformed lamellar structure with numerous low-angle boundaries (LAGs), while the brass layer shows an annealed structure consisting of many equiaxed recrystallization grains. The average grain size for the brass layer is ~3.6 μm. The discrepant structures of the copper and brass layers are ascribed to the low recrystallization driving force of the deformed coarse-grained copper, as has been reported in previous studies [16,17]. Figure 4c shows that the hardness value of the copper layer is about 100 HV, which is lower than that of the brass layer (130 HV). This is a typical multilayered soft–hard structure. As reported by Huang et al. [13] and Li et al. [16], the multilayered soft–hard metallic blocks always exhibit a good combination of strength and ductility. As shown in Figure 5a, the presented multilayered soft–hard copper–brass block also shows a high yield strength of ~320 MPa and good uniform elongation of ~20%, which is superior to the mechanical properties of copper–brass layer and the related materials, as already summarized by Huang et al. [13]. In this study, the impact energies of the soft–hard copper–brass block were evaluated under different testing temperatures (LNT, RT, and 200 °C). Figure 5b shows that the highest impact resistance with the impact energy of 8.15 J was achieved at LNT. When the testing temperature increased up to RT, the impact energy was 7.39 J. As the testing temperature increased up to 200 °C, the soft–hard copper–brass block showed a further decrease in impact resistance, and the impact energy reached 7.04 J. The detailed explanation for the relationship between the impact energy and testing temperature can be revealed by further exploring the fracture morphologies and coordinated deformation behavior in the following section.

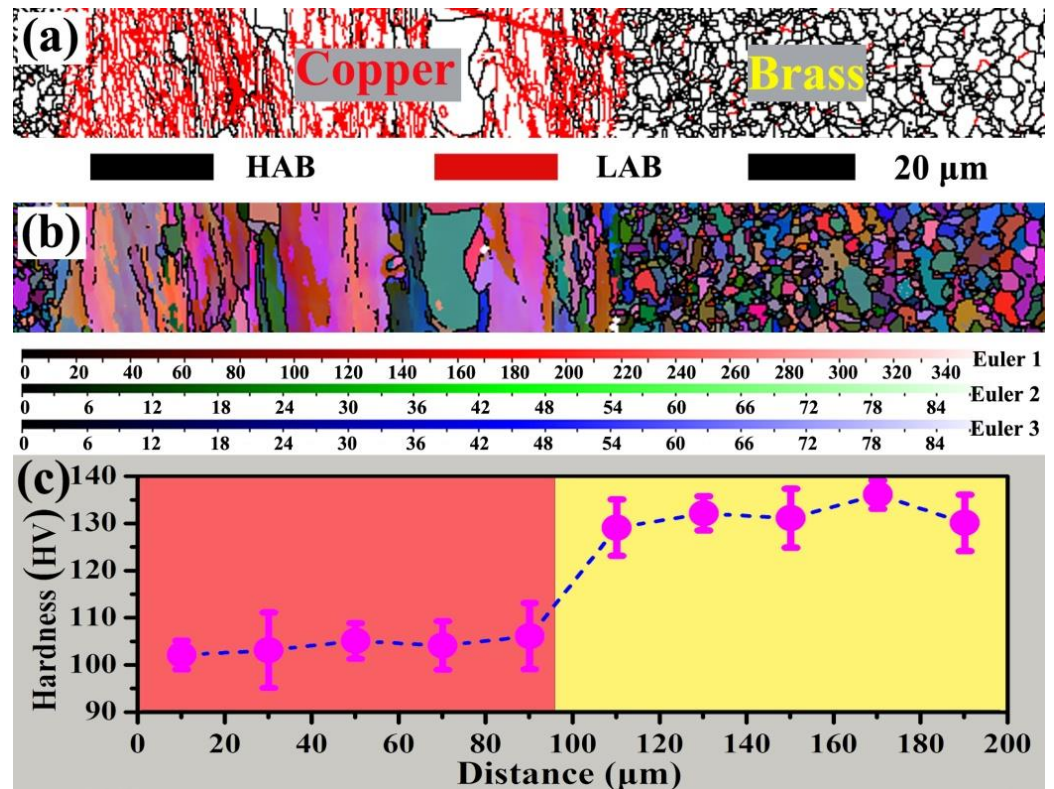


**Figure 4.** (a) The distributions of the low-angle boundaries (LAGs, misorientation of 2–15°) and high angle-boundaries (HAGs, misorientation of >15°) for the copper–brass block. (b) A Euler map of the cross-sectional copper–brass block. (c) The hardness distribution of the cross-section of copper–brass block.

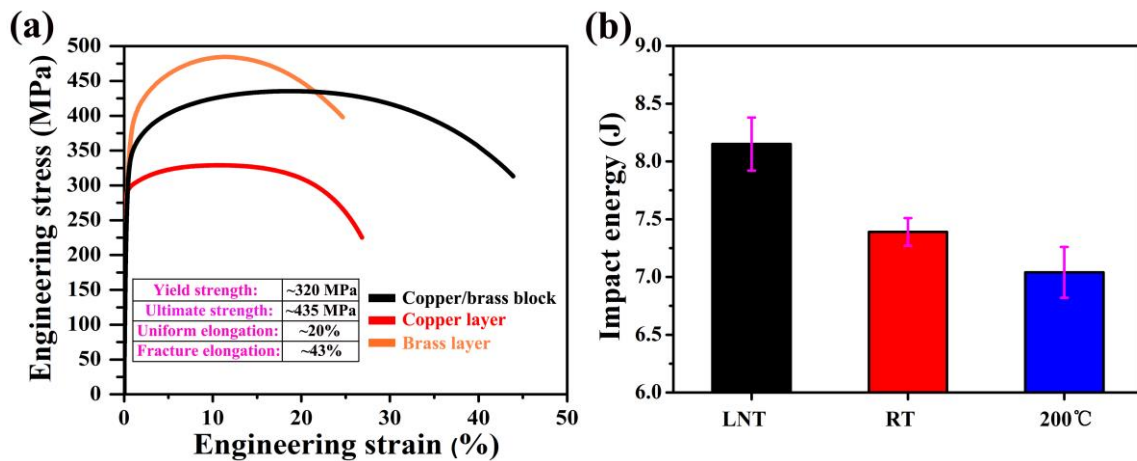


**Figure 5.** (a) The engineering stress–strain curves of the copper layer, brass layer, and multilayered soft–hard copper–brass block. (b) The impact energies of the present multilayered soft–hard copper–brass block tested at various temperatures.

Figure 6 shows the cross-sectional fracture morphologies around the V-notch for the multilayered soft–hard copper–brass blocks impacted at LNT, RT, and 200 °C. It is noted that all of the impacted samples presented a similar V-crack morphology. The copper and brass layers near the roots of the V-notches were cracked using a high-speed impacting load, while the copper and brass layers far away from the roots of the V-notches suffered from a decreased impacting load and were just bent. In addition, an evident delamination of the copper–brass interface around the root of the V-crack can be found for all impacted samples. Figure 7 clearly indicates that the delamination lengths of copper–brass interface

for all impact specimens are nearly identical. As indicated by Osman et al. [19] and Cepeda-Jiménez et al. [22], dissimilar metal blocks with ultrafine laminate structures often show excellent impact toughness, which can be ascribed to the extra delamination of hetero-interfaces, consuming the high plastic deformation energy. The density of the hetero-interfaces will play an important role in determining the impact toughness. Theoretically speaking, a copper–brass block with a thinner layer thickness will have a higher density of hetero-interfaces and will be more likely to achieve a better impact toughness because of the coordinated deformation effects of the numerous hetero-interfaces. In addition, the well-bonded interfaces can accelerate the coordinated deformation effects [16]. A combination of suitable pressure ( $\sim 0.5\text{--}50$  MPa) and a high temperature ( $\sim 0.5\text{--}0.8$  Tm) can improve the metallurgical bonding between the copper and brass layers, which may enhance the bonding strength for copper–brass interfaces [16] so as to improve the impact toughness. In this work, although the testing temperatures were altered, the cracked brass layers tested at LNT, RT, and  $200^\circ\text{C}$  showed semblable fracture surfaces with many dimples, and the cracked copper layers tested under LNT, RT and  $200^\circ\text{C}$  also show semblable, brittle fracture surfaces (Figure 8a–f). The similar fracture morphologies of the copper–brass layers under various testing temperatures can be ascribed to the impact toughness of metals with FCC crystal lattices, which are usually insensitive to the environmental temperature [20,21]. Thus, there must be other factors that can affect the impact toughness of the present soft–hard copper–brass blocks. As shown in Figure 8g,h, the tiny dimples found on the delaminated surface of copper–brass interface at RT and LNT were denser, which may indicate more energy consumption. Generally speaking, energy consumption around hetero-interfaces is always related to coordinated plastic deformation. For the present copper–brass interfaces, the brass had a nearly dislocation-free structure, which was believed to make a great contribution to the energy consumption. The deformed structures of coarse-grained brass around the delamination copper–brass interfaces are displayed in Figure 9. It shows that the deformation twins decrease with the increase in testing temperature. As confirmed by previous studies [17,23,24], deformation twins are inclined to be formed at high strain rates from the high-speed impact load, especially at low temperatures, and may consume more deformation energy and enhance the impact toughness of the metals. This may be the reason that the impact energy at LNT is higher than that at RT. As compared in Figure 8g–i, the fracture morphology of the delaminated soft–hard interface at  $200^\circ\text{C}$  shows scarce dimples, which may indicate a mild plastic deformation of the copper–brass interfaces. Kulagin et al. [25] and Malik et al. [26] have indicated that the grain boundaries and phase interfaces were weak when a sample was heated at high temperatures. In fact, the grain boundaries and phases are believed to be special structures, which are composed of many defects (vacancies, dislocations, micro-holes, etc.). These special structures usually have a lower softening temperature, which is caused by recovery and recrystallization. Thus, the impact energy of copper–brass at  $200^\circ\text{C}$  has the lowest impact resistance, and the impact energy or toughness is decreased with the increase in testing temperature.

Although this work has systematically explored the effects of three kinds of typical testing temperatures on the impact properties of a copper–brass block with a layer thickness of  $\sim 100\ \mu\text{m}$ , some other influences, such as the layer thickness and preparation factors, have been ignored. These will be further revealed in future studies, which may provide more precise theoretical guidance for the industrial applications of copper–brass blocks.

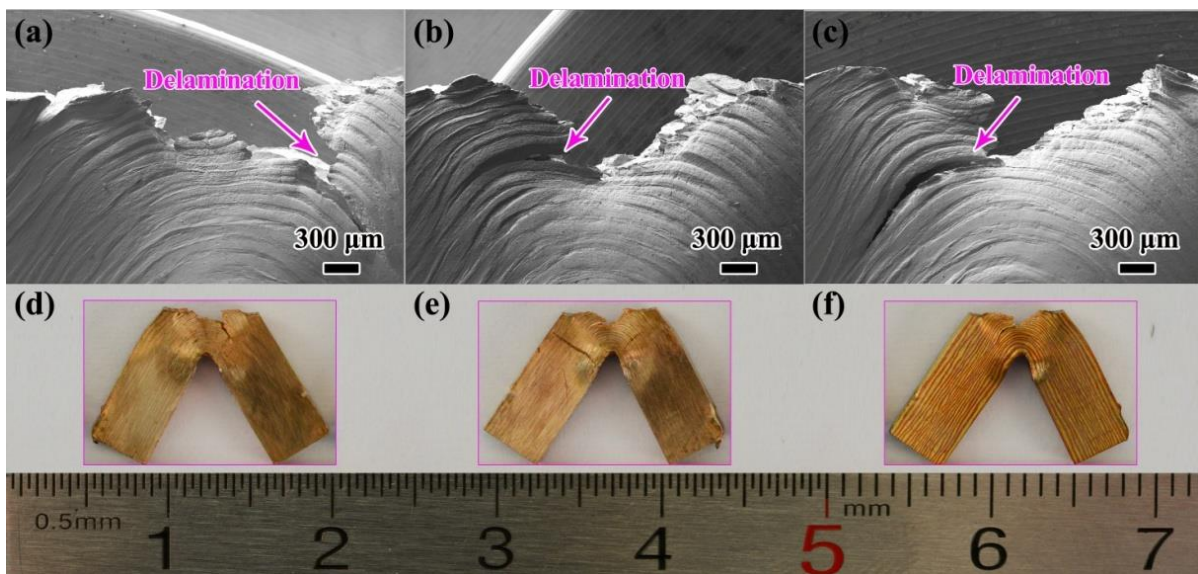


**Figure 6.** The images of the impacted copper–brass blocks at different temperatures: (a–c) the SEM images around the V-notch for fractured copper–brass blocks at LNT, RT, and 200 °C, respectively; (d–f) the optical images for fractured copper–brass blocks at LNT, RT, and 200 °C, respectively.

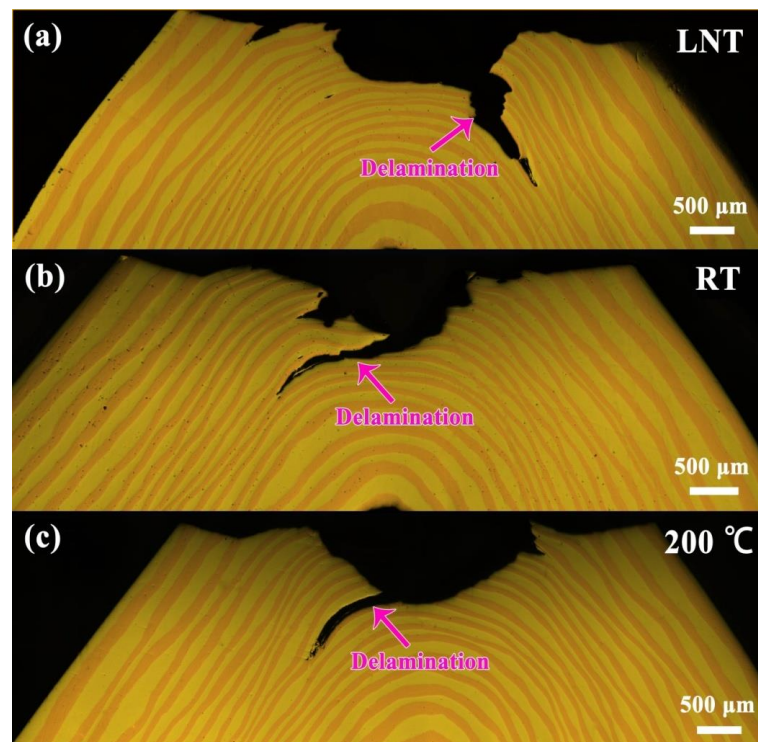


**Figure 7.** (a–c) The cross-sectional optical images of the multilayered copper–brass blocks impacted at LNT, RT, and 200 °C, respectively. It is noted that the cross-section is selected in the mid-plane along the thickness direction.

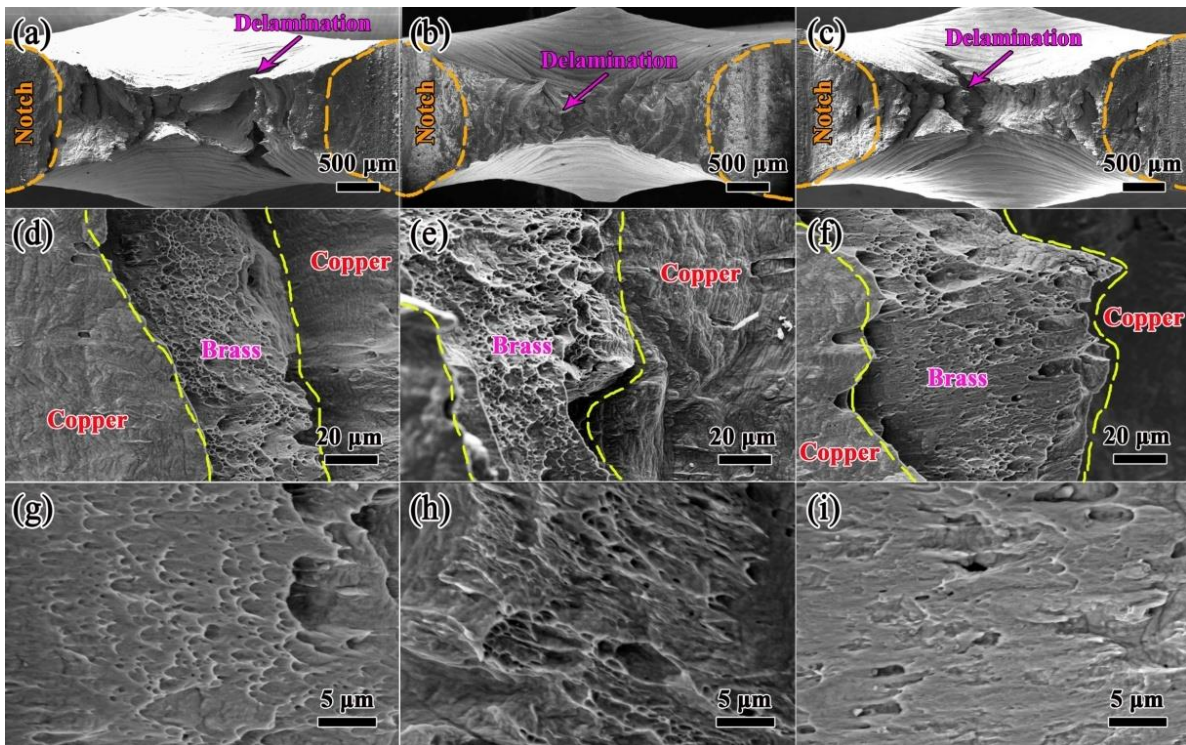


**Figure 8.** (a–c) The fracture surfaces of the copper–brass blocks impacted at LNT, RT, and 200 °C, respectively. (d–f) The fracture morphologies of the copper and brass layers at LNT, RT, and 200 °C, respectively. (g–i) The morphologies of the delaminated copper–brass interfaces at LNT, RT, and 200 °C, respectively.

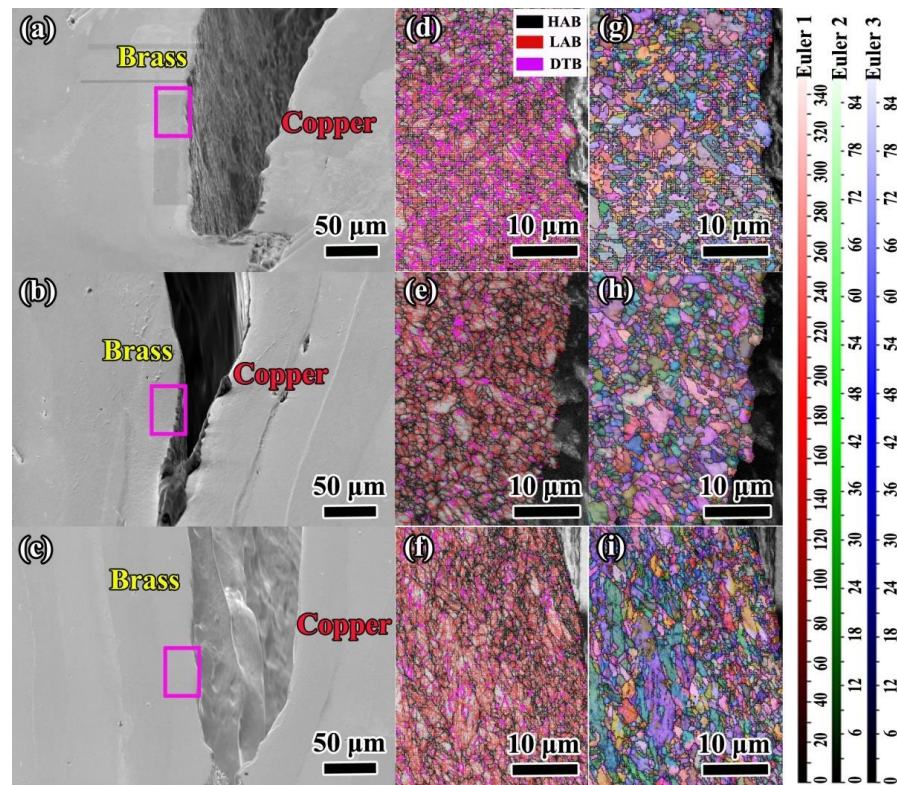


**Figure 9.** (a–c) The SEM images of delaminated copper–brass interfaces at LNT, RT, and 200 °C, respectively. (d–f) The distributions of LAGs, HAGs, and deformed twin boundaries (DTBs) of the selected regions in (a–c), respectively. (g–i) The Euler maps of the selected regions in (a–c), respectively.



#### 4. Conclusions

In summary, a combined DWFA technique was employed to successfully prepare a copper–brass block with a soft–hard multilayered structure. The influence of the testing temperature on the impact properties was revealed. Some conclusions were drawn, as follows:

1. The impact energies of the present multilayered soft–hard copper–brass blocks tested at LNT, RT, and 200 °C were 8.15 J, 7.39 J, and 7.04 J, respectively, which indicated that the impact energy was positively dependent on the testing temperature;
2. The copper–brass layers that cracked under various testing temperatures show similar fracture morphologies. This can be ascribed to the fracturing of metals with a FCC crystal lattice usually being insensitive to the environmental temperature;
3. The highest impact energy at LNT was attributed to the high density of tiny dimples caused by coordinated plastic deformation effects during the delamination of the soft–hard copper–brass interfaces. The high temperature of 200 °C can weaken the copper–brass interface, reduce the absorption of the deformation energy, and lead to decreased impact resistance.

**Author Contributions:** Investigation, T.L., K.L., M.W. and Q.Y.; formal analysis, J.L., Q.M., M.C. and Y.S.; resources, Z.Z. and Y.Z.; methodology, Q.M. and Y.W.; writing—original draft, T.L.; writing—review and editing, Y.Z., Q.M. and J.L. All authors have read and agreed to the published version of the manuscript.

**Funding:** The authors acknowledge the financial support of the Natural Science Foundation of Anhui Province (2208085QE125), the National Natural Science Foundation of China (52101030), the Scientific Research Starting Foundation of Anhui Polytechnic University (2020YQQ026, S022021005), the Innovation and Entrepreneurship Training Program for College Students of Anhui Province (S202110363167, S202110363174), and the Scientific Research Foundation of Anhui Polytechnic University of China (Xjky2022024).

**Institutional Review Board Statement:** Not applicable.

**Informed Consent Statement:** Not applicable.

**Data Availability Statement:** The data presented in this study are available on request from the corresponding authors.

**Conflicts of Interest:** The authors declare no conflict of interest.

#### References

1. Liang, N.N.; Liu, J.Z.; Lin, S.C.; Wang, Y.; Wang, J.T.; Zhao, Y.H.; Zhu, Y.T. A multiscale architected CuCrZr alloy with high strength, electrical conductivity and thermal stability. *J. Alloys Comp.* **2018**, *735*, 1389–1394. [\[CrossRef\]](#)
2. Lu, X.K.; Zhao, Y.; Wang, G.; Zhu, X.B. Effects of structure characteristics and fluid on the effective thermal conductivity of sintered copper foam. *Results Phys.* **2020**, *19*, 103655. [\[CrossRef\]](#)
3. Mao, Q.Z.; Zhang, Y.S.; Liu, J.Z.; Zhao, Y.H. Breaking material property trade-offs via macrodesign of microstructure. *Nano Lett.* **2021**, *21*, 3191–3197. [\[CrossRef\]](#) [\[PubMed\]](#)
4. Mao, Q.Z.; Zhang, Y.S.; Guo, Y.Z.; Zhao, Y.H. Enhanced electrical conductivity and mechanical properties in thermally stable fine-grained copper wire. *Commun. Mater.* **2021**, *2*, 46. [\[CrossRef\]](#)
5. Liang, N.N.; Zhao, Y.H.; Wang, J.T.; Zhu, Y.T. Effect of grain structure on Charpy impact behavior of copper. *Sci. Rep.* **2017**, *7*, 44738. [\[CrossRef\]](#)
6. An, X.H.; Lin, Q.Y.; Wu, S.D.; Zhang, Z.F. Improved fatigue strengths of nanocrystalline Cu and Cu–Al Alloys. *Mater. Res. Lett.* **2015**, *3*, 135–141. [\[CrossRef\]](#)
7. Shirdel, M.; Mirzadeh, H.; Parsa, M.H. Nano/ultrafine grained austenitic stainless steel through the formation and reversion of deformation-induced martensite: Mechanisms, microstructures, mechanical properties, and TRIP effect. *Mater. Charact.* **2015**, *103*, 150–161. [\[CrossRef\]](#)
8. Straumal, B.B.; Pontikis, V.; Kilmametov, A.R.; Mazilkin, A.A.; Dobatkin, S.V.; Baretzky, B. Competition between precipitation and dissolution in Cu–Ag alloys under high pressure torsion. *Acta Mater.* **2017**, *122*, 60–71. [\[CrossRef\]](#)
9. Tajally, M.; Huda, Z.; Masjuki, H.H. A comparative analysis of tensile and impact-toughness behavior of cold-worked and annealed 7075 aluminum alloy. *Inter. J. Impact Eng.* **2010**, *37*, 425–432. [\[CrossRef\]](#)

10. Ma, X.L.; Huang, C.X.; Xu, W.Z.; Zhou, H.; Wu, X.L.; Zhu, Y.T. Strain hardening and ductility in a coarse-grain/nanostructure laminate material. *Scr. Mater.* **2015**, *103*, 57–60. [[CrossRef](#)]
11. Wang, Y.F.; Yang, M.X.; Ma, X.L.; Wang, M.S.; Yin, K.; Huang, A.H.; Huang, C.X. Improved back stress and synergetic strain hardening in coarse-grain/nanostructure laminates. *Mater. Sci. Eng. A* **2018**, *727*, 113–118. [[CrossRef](#)]
12. Ma, X.L.; Huang, C.X.; Moering, J.; Ruppert, M.; Hoppel, H.W.; Goken, M.; Narayan, J.; Zhu, Y.T. Mechanical properties of copper/bronze laminates: Role of interfaces. *Acta Mater.* **2016**, *116*, 43–52. [[CrossRef](#)]
13. Huang, C.X.; Wang, Y.F.; Ma, X.L.; Yin, S.H.; Hoppel, W.; Goken, M.; Wu, X.L.; Gao, H.J.; Zhu, Y.T. Interface affected zone for optimal strength and ductility in heterogeneous laminate. *Mater. Today* **2018**, *21*, 713–719. [[CrossRef](#)]
14. Huang, M.; Xu, C.; Fan, G.H.; Maawad, E.; Gan, W.M.; Geng, L.; Lin, F.X.; Tang, G.Z.; Wu, H.; Du, Y.; et al. Role of layered structure in ductility improvement of layered Ti-Al metal composite. *Acta Mater.* **2018**, *153*, 235–249. [[CrossRef](#)]
15. Qin, W.B.; Mao, Q.Z.; Kang, J.J.; Liu, Y.Y.; Shu, D.F.; She, D.S.; Liu, Y.F.; Li, J.S. Superior impact property and fracture mechanism of a multilayered copper/bronze laminate. *Mater. Lett.* **2019**, *250*, 60–63. [[CrossRef](#)]
16. Li, J.S.; Wang, S.Z.; Mao, Q.Z.; Huang, Z.W.; Li, Y.S. Soft/hard copper/bronze laminates with superior mechanical properties. *Mater. Sci. Eng. A* **2019**, *756*, 213–218. [[CrossRef](#)]
17. Liu, T.; Gu, C.Y.; Li, J.S.; Zhou, Z.C.; Lu, Y.; Gao, F.; Chen, M.; Mao, Q.Z.; Lu, X.K.; Li, Y.S. Effect of structural orientation on the impact properties of a soft/hard copper/brass laminate. *Vacuum* **2021**, *191*, 110388. [[CrossRef](#)]
18. Zhu, Y.T.; Wu, X.L. Perspective on hetero-deformation induced (HDI) hardening and back stress. *Mater. Res. Lett.* **2019**, *7*, 393–398. [[CrossRef](#)]
19. Osman, T.M.; Hassan, H.A.; Lewandowski, J.J. Interface effects on the quasi-static and impact toughness of discontinuously reinforced aluminum laminates. *Metall. Mater. Trans. A* **2008**, *39A*, 1993–2006. [[CrossRef](#)]
20. Ibrahim, O.H.; Ibrahim, I.S.; Khalifa, T.A.F. Impact behavior of different stainless steel weldments at low temperatures. *Eng. Fail. Anal.* **2010**, *17*, 1069–1076. [[CrossRef](#)]
21. Smirnov, I.; Konstantinov, A. Influence of ultrafine-grained structure produced by equal-channel angular pressing on the dynamic response of pure copper. *Procedia Struct. Integrity* **2018**, *13*, 1336–1341. [[CrossRef](#)]
22. Cepeda-Jiménez, C.M.; García-Infanta, J.M.; Pozuelo, M.; Ruano, O.A.; Carreño, F. Impact toughness improvement of high-strength aluminum alloy by intrinsic and extrinsic fracture mechanisms via hot rolling bonding. *Scr. Mater.* **2009**, *61*, 407–410. [[CrossRef](#)]
23. Gludovatz, B.; Hohenwarter, A.; Thurston, K.V.S.; Bei, H.; Wu, Z.; George, E.P.; Ritchie, R.O. Exceptional damage-tolerance of a medium-entropy alloy CrCoNi at cryogenic temperatures. *Nat. Commun.* **2015**, *7*, 10602. [[CrossRef](#)] [[PubMed](#)]
24. Hasan, M.N.; Liu, Y.F.; An, X.H.; Gu, J.; Song, M.; Cao, Y.; Li, Y.S.; Zhu, Y.T.; Liao, X.Z. Simultaneously enhancing strength and ductility of a high-entropy alloy via gradient hierarchical microstructures. *Inter. J. Plast.* **2019**, *123*, 178–195. [[CrossRef](#)]
25. Kulagin, R.; Beygelzimer, Y.; Ivanisenko, Y.; Mazilkin, A.; Straumal, B.; Hahn, H. Instabilities of interfaces between dissimilar metals induced by high pressure torsion. *Mater. Lett.* **2018**, *222*, 172–175. [[CrossRef](#)]
26. Malik, A.; Chaudry, U.M.; Hamad, K.; Jun, T.S. Microstructure features and superplasticity of extruded, rolled and SPD-processed magnesium alloys: A short review. *Metals* **2021**, *11*, 1766. [[CrossRef](#)]